PNAS RESEARCH ARTICLE | IMMUNOLOGY AND INFLAMMATION

ROCK2 interacts with p22phox to phosphorylate p47phox and to control NADPH oxidase activation in human monocytes

Asma Tlili[a,1], Coralie Pintard[a,1], Margarita Hurtado-Nedelec[a,b], Dan Liu[a,c], Viviana Marzaioli[a,d], Nathalie Thieblemont[a], Pham My-Chan Dang[a], and Jamel El-Benna[a,2]

Edited by Jean-Laurent Casanova, The Rockefeller University, New York, NY; received May 27, 2022; accepted December 12, 2022

Monocytes play a key role in innate immunity by eliminating pathogens, releasing high levels of cytokines, and differentiating into several cell types, including macrophages and dendritic cells. Similar to other phagocytes, monocytes produce superoxide anions through the NADPH oxidase complex, which is composed of two membrane proteins (p22phox and gp91phox/NOX2) and four cytosolic proteins (p47phox, p67phox, p40phox and Rac1). The pathways involved in NADPH oxidase activation in monocytes are less known than those in neutrophils. Here, we show that p22phox is associated with Rho-associated coiled-coil kinase 2 (ROCK2) in human monocytes but not neutrophils. This interaction occurs between the cytosolic region of p22phox (amino acids 132 to 195) and the coiled-coil region of ROCK2 (amino acids 400 to 967). Interestingly, ROCK2 does not phosphorylate p22phox, p40phox, p67phox, or gp91phox in vitro but phosphorylates p47phox on Ser304, Ser315, Ser320 and Ser328. Furthermore, KD025, a selective inhibitor of ROCK2, inhibited reactive oxygen species (ROS) production and p47phox phosphorylation in monocytes. Specific inhibition of ROCK2 expression in THP1-monocytic cell line by siRNA inhibited ROS production. These data show that ROCK2 interacts with p22phox and phosphorylates p47phox, and suggest that p22phox could be a shuttle for ROCK2 to allow p47phox phosphorylation and NADPH oxidase activation in human monocytes.

monocyte | NADPH oxidase/NOX2 | ROCK2 | p22phox | p47phox

Phagocytic cells, including monocytes, macrophages, and neutrophils, are key cells of host defense against pathogens, such as bacteria and fungi (1). During infection or inflammation, circulating monocytes migrate to the infected tissues where they phagocytose and kill the microbes, produce high quantities of cytokines, and differentiate into specific subsets of macrophage types and dendritic cells (2).

The microbicidal and inflammatory functions of monocytes are based on the production of reactive oxygen species (ROS), such as superoxide anions, hydrogen peroxide, hydroxyl radicals, and hypochloric acid (3). The first step in the generation of ROS is the production of the superoxide anions, which are the precursor of the other ROS molecules. In phagocytes, the enzyme responsible for superoxide anion production is the phagocyte Nicotinamide adenine dinucléotide phosphate H+ (NADPH) oxidase (4, 5). This enzyme is composed of two membrane proteins (p22phox and gp91phox/NOX2) and four cytosolic proteins (p47phox, p67phox, p40phox, and rac1/2), which assemble to form an active enzyme (6, 7). NADPH oxidase activation is accompanied by the phosphorylation of p47phox, p67phox, p40phox, p22phox, and gp91phox proteins (8). The phosphorylation of p47phox plays a key role in NADPH oxidase activation (9). The pathways involved in NADPH oxidase activation and ROS production are widely studied in neutrophils, however, less is known in monocytes. Recently, it was shown that EROS (Essential for ROS) protein, also called CYBC1 or C17orf62, is a novel regulator of the NADPH oxidase in human and mice phagocytes (10, 11). To further investigate the pathways involved in NADPH oxidase activation in monocytes, we sought to identify the proteins that interact with one of the key membrane subunits of the enzyme complex, the p22phox.

Human p22phox is a 195-amino acid protein consisting of a short N-terminal tail, four trans-membrane domains and a long C-terminal tail ranging from amino acids 130 to 195 (6, 12, 13). In resting cells, p22phox interacts with gp91phox via the transmembrane spanning domains to stabilize the complex (12, 13). During activation, the intracellular cytosolic tail of p22phox (amino acids 130 to 190) interacts with p47phox via a p22phox-proline rich region (PRR) and the p47phox-SH3 domains (14–17).

Rho-associated coiled-coil kinases 1 and 2 (ROCK1 and ROCK2) are serine/threonine protein kinases and the effectors of Rho GTPase (18). ROCK1 and ROCK2 are 1,354 and 1,388-amino acid proteins, respectively, and have a molecular weight of 158 kDa and 160 kDa, respectively. Structurally, they have a kinase domain, a coiled-coil region, a

Significance

Monocytes play a key role in innate immunity and inflammation by producing reactive oxygen species (ROS). The enzyme responsible for ROS production is the phagocyte NADPH oxidase, which is composed of two membrane proteins (p22phox and gp91phox/NOX2) and four cytosolic proteins (p47phox, p67phox, p40phox, and Rac1/2). Here, we show that p22phox associates with Rho-associated coiled-coil kinase 2 (ROCK2) in human monocytes. Interestingly, ROCK2 does not phosphorylate p22phox, p40phox, p67phox or gp91phox in vitro but highly phosphorylates p47phox. Furthermore, selective inhibition of ROCK2 activity and expression, inhibited both ROS production and p47phox phosphorylation in human monocytes. These data identify a key role of ROCK2 in the regulation of ROS production by monocytes. The ROCK2-p22phox interaction could be used to target monocyte ROS production.

Author contributions: P.M.-C.D and J.E.-B designed research; A.T., C.P., M.H.-N., D.L., V.M., N.T., and J.E.-B. performed research; A.T., C.P., M.H.-N., D.L., V.M., N.T., P.M.-C.D., and J.E.-B. analyzed data; and A.T., C.P., M.H.-N., V.M., N.T., P.M.-C.D., and J.E.-B. wrote the paper.

The authors declare no competing interest.

This article is a PNAS Direct Submission.

[1]A.T. and C.P. contributed equally to this work.

[2]To whom correspondence may be addressed. Email: jamel.elbenna@inserm.fr.

This article contains supporting information online at https://www.pnas.org/lookup/suppl/doi:10.1073/pnas.2209184120/-/DCSupplemental.

Published January 10, 2023.

Rho-binding domain (RBD), a pleckstrin homology (PH) domain, and several phosphorylated sites (18–20). ROCK1 and ROCK2 share 65% overall identity in amino acid sequences with the highest homology (92%) within the kinase domains, while they display significant diversity in the coiled-coil regions and in the PH domain, as the identity is only 55% and 65%, respectively (18, 21). They are involved in several cellular functions, such as cytoskeleton rearrangement, apoptosis, cell adhesion, phagocytosis, proliferation, and migration (22–25). The development of selective and nonselective ROCK inhibitors as therapeutic agents for hypertension (26) and cardiovascular diseases is booming (27, 28). Two inhibitors are primarily used as research tools, Y27632, which inhibits both ROCK1 and ROCK2, and KD025, a more selective inhibitor for ROCK2 (29).

We hypothesized that p22phox could interact with unidentified partners in resting human monocytes. To identify these partners, we performed immunoprecipitation using a specific antibody directed against the last 10 C-terminal amino acids of p22phox and analyzed the bound proteins by mass spectrometry. We identified ROCK2 as a p22phox-interacting protein and showed its involvement in NADPH oxidase activation and ROS production in human monocytes.

Results

Identification of ROCK2 as a p22phox-Interacting Protein in Human Monocytes and Monocyte-Derived Dendritic Cells but Not in Neutrophils. To identify regulators of NADPH oxidase in human monocytes, p22phox was immunoprecipitated from resting human monocytes lysates, and bound proteins were identified by mass spectrometry analysis. The results showed that, as expected, the cytochrome b558 heavy chain (gp91phox/NOX2) coimmunoprecipitated with p22phox identified with a Mascot score of 221 (*SI Appendix,* Table S1). Interestingly, the highest Mascot score and the highest number of peptides obtained during this analysis corresponded to Rho-associated protein kinase 2 (ROCK2), suggesting an interaction between p22phox and ROCK2. The Mascot score of ROCK2 is 363, with all the 34 identified peptides belonging to the ROCK2 sequence and 30 peptides being specific for ROCK2, thus corresponding to a high level of confidence. In contrast, only four peptides were common to ROCK2 and ROCK1 and none of the identified peptides were specific for ROCK1 (*SI Appendix*, Table S2 and Fig. S1), therefore, the interaction of p22phox with ROCK1 seems unlikely, given that the Mascot score of ROCK1 is 18, equal to the one found with control IgG.

Western blot analysis confirmed the presence of ROCK2 in human monocytes, which was also expressed in monocyte-derived dendritic cells (Mo-DC) and in human neutrophils (Fig. 1*A*). To confirm the p22phox/ROCK2 interaction in human monocytes, coimmunoprecipitation experiments were performed (Fig. 1*B*). The results showed that ROCK2 was detected in the p22phox immunoprecipitated sample from monocytes (IP-p22phox) but not in the IgG control immunoprecipitated fraction (IP-Ctrl). The total monocyte lysates showed the levels of ROCK2 and p22phox protein expression. As expected, the gp91phox protein was present in the p22phox-immunoprecipitated sample. In addition, we also observed a coimmunoprecipitation of ROCK2 and gp91phox with p22phox in Mo-DC, (Fig. 1*C*). Surprisingly, ROCK2 did not coimmunoprecipitate with p22phox in human neutrophils (Fig. 1*D*), and as expected the gp91phox protein was present in the p22phox-immunoprecipitated sample. Interestingly, immunoprecipitation of ROCK2 using two different commercial antibodies showed the presence of p22phox in the immunoprecipitate (Fig. 1*E*). These results suggest that the p22phox/ROCK2 interaction occurs in monocytes and Mo-DC but not in neutrophils and could be cell specific.

Direct Interaction of ROCK2 and p22phox Proteins. To investigate whether the interaction between ROCK2 and p22phox is direct or occurs via a bridging partner, we used purified recombinant proteins and dot-blot assays. The entire ROCK2 protein is composed of 1,388 amino acids and has a molecular weight of 160 kDa with different domains (Fig. 2*A*). This high molecular weight protein cannot be expressed in bacteria. We thus used different constructs of the ROCK2 protein (amino acids 11 to 552, amino acids 400 to 967, amino acids 968 to 1,388) to study the interaction with p22phox and to map the interacting region. These fragments were amplified by PCR and cloned into the pGEX plasmid. Then, the fragments were transformed into *Escherichia coli* BL21 for protein expression and purification and assessed by Coomassie blue staining (Fig. 2*B*). To determine whether ROCK2 interacted directly and specifically with p22phox and to identify the interaction region, a dot-blot assay was performed using recombinant His-ROCK2 (11 to 552), ROCK2 (400 to 967), ROCK2 (968 to 1,388), and GST-p22phox (132 to 195) as well as Bovine serum albumin (BSA) and Glutathion S-transferase (GST) as control proteins. The proteins were applied to a nitrocellulose membrane and then probed with the recombinant protein GST-p22phox (132 to 195). Interaction was detected with a mouse anti-p22phox antibody and a secondary antibody HRP-conjugated goat anti-mouse. The results showed that p22phox interacted with the ROCK2 (400 to 967) fragment but not with His-ROCK2 (11 to 552) or ROCK2 (968 to 1,388) (Fig. 2*C*). The intensive spot of the positive control (GST-p22phox) confirmed the detection assay, and no signal spot was detected for the negative controls (BSA and GST), indicating that the interaction of p22phox with ROCK2 is specific (Fig. 2*C*). These results clearly demonstrate a direct interaction between ROCK2 and p22phox and that the interaction is localized in the coiled-coil region of ROCK2 (amino acids 400 to 967).

ROCK2 Colocalizes with p22phox in Human Monocytes. P22phox is a membrane protein known to be localized in the plasma membrane and membranes of granules in phagocytes. To address whether ROCK2 is localized in the same cell fraction as p22phox, we analyzed their localization. First, resting and stimulated monocytes were fractionated into cytosol and membrane fractions, and proteins were detected. Intercellular adhesion molecule 1 (ICAM1), a known membrane protein, and GAPDH (Glyceraldehyde-3-phosphate dehydrogenase), a known cytosolic protein, were used as specific membrane and cytosolic markers, respectively. As expected, ICAM1 and p22phox were present exclusively in the membranes fraction, GAPDH was present exclusively in the cytosolic fraction and p47phox was mostly present in the cytosolic fraction (Fig. 3*A*). Interestingly, ROCK2 was localized in the cytosol and membrane fractions of resting, formyl-methionyl-leucylphenylalanine (fMLF)- and phorbol-12-myristate-13-acetate (PMA)-stimulated human monocytes, although the molecular weight was slightly different in some membranes fractions (Fig. 3*A*). Quantification data showed that membrane ROCK2 represents 60 to 75% of the cytosolic ROCK2 (Fig. 3*B*).

Second, confocal microscopy analysis was performed to identify and confirm the localization of ROCK2 and its colocalization with p22phox in resting monocytes. Confirming the above results, ROCK2 localized mostly in the cytoplasm and plasma membrane in resting monocytes, whereas p22phox localized exclusively at the plasma and granule membranes (Fig. 3*C*). These results show

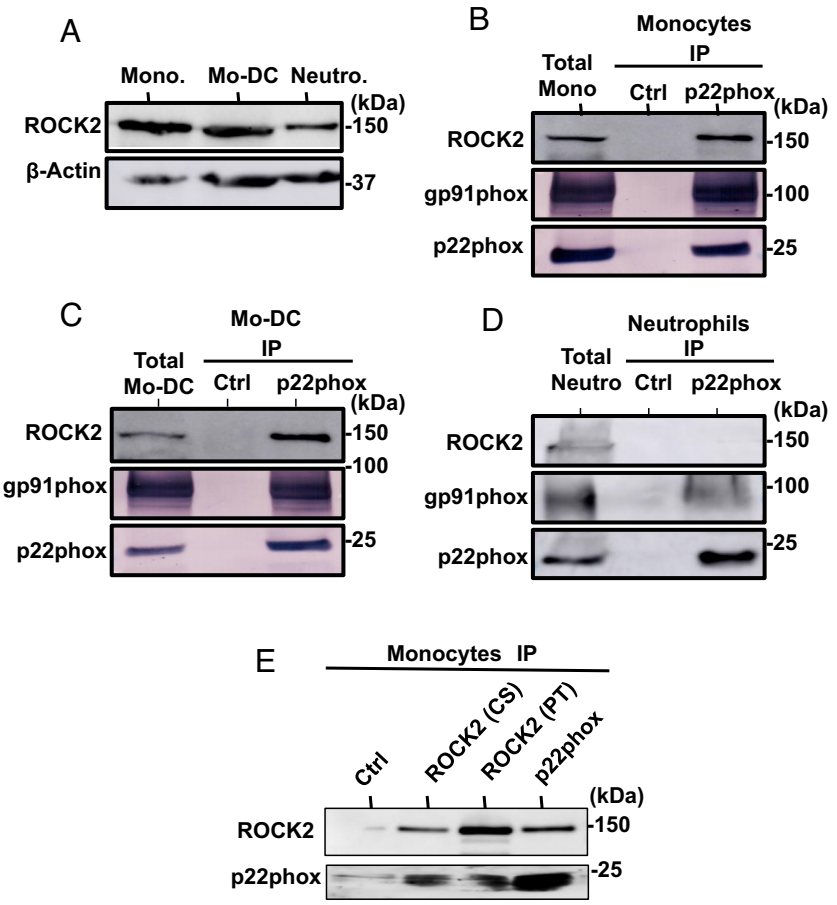

Fig. 1. ROCK2 protein is expressed in phagocytes and interacts with p22phox in monocytes. (*A*) Western blot of ROCK2 and β-actin in human monocytes (Mono), Mo-DC, and human neutrophils (Neutro). Representative western blots of co immunoprecipitation (co-IP) of ROCK2 and gp91phox with p22phox in monocytes (*B*), dendritic cells (*C*), and neutrophils (*D*). The p22phox-immunoprecipitated fraction (IP-p22phox) and IP-IgG-control-immunoprecipitated fractions (IP-IgG-Ctrl) were analyzed by SDS-PAGE and western blots and proteins detected with anti-ROCK2, anti-gp91phox, and anti-p22phox antibodies. The total monocytes (Total mono), total dendritic cells (Total Mo-DC), and total neutrophils (Total neutro) show ROCK2 and p22phox protein levels. (*E*) ROCK2 was immunoprecipitated using ROCK2-specific antibodies from Cell Signaling (CS), ProteinTech (PT), or control IgG (Ctrl), and immunoprecipitated fractions were analyzed by SDS-PAGE and western blots and proteins detected with anti-ROCK2 and anti-p22phox antibodies. Western blots are a representative example of three independent experiments.

a colocalization of ROCK2 and p22phox (Merge) in human monocytes, further supporting their interaction.

ROCK2 Phosphorylates p47phox In Vitro and in Human Monocytes. To investigate whether ROCK2 can phosphorylate p22phox and/or the other NADPH oxidase proteins, active recombinant ROCK2 fragment was incubated with recombinant p22phox-cytosolic tail (amino acids 132-195), recombinant p40phox, recombinant p67phox, recombinant gp91phox-cytosolic tail (amino acids 291-570), and recombinant p47phox in the absence or presence of Adenosine triphosphate (ATP). Then, the reaction was stopped by protein denaturation, and the proteins were analyzed by western blots using an anti-phospho antibody known to recognize phosphorylated-Ser/Thr by ROCK2 (30, 31). Surprisingly, the results showed that ROCK2 did not phosphorylate its partner p22phox (Fig. 4*A*), neither p40phox (Fig. 4*B*), p67phox (Fig. 4*C*), nor gp91phox (Fig. 4*D*) but clearly phosphorylated p47phox (Fig. 4*E*). To determine the p47phox phosphorylated sites, we used specific anti-phospho-serine-p47phox antibodies we have previously developed (32, 33). The results show that ROCK2 phosphorylates p47phox on Ser304 (Fig. 4*F*), Ser315 (Fig. 4*G*), Ser320 (Fig. 4*H*), and Ser328 (Fig. 4*I*). The use of a rabbit nonimmune IgG control showed no p47phox phosphorylation, thus demonstrating the specificity of the anti-phospho antibodies (Fig. 4*J*).

To further investigate whether ROCK2 could phosphorylate p47phox in intact monocytes, we first measured ROCK2 activation in human monocytes using an antibody against its known endogenous substrate, the myosin phosphatase targeting 1 (MYPT1) (34). Results showed that MYPT1 is constitutively phosphorylated in resting cells and stimulation of monocytes did not affect this process (*SI Appendix*, Fig. S2), thus suggesting that ROCK2 is constitutively active in resting monocytes. Freshly isolated human monocytes were treated with Y27632, a ROCK1/2 inhibitor, or KD025, a selective ROCK2 inhibitor, prior to stimulation with fMLF, PMA or opsonized zymosan. Interestingly, ROCK2 inhibitors altered the phosphorylation of p47phox on Ser304, Ser315, Ser320, and Ser328 in fMLF- and opsonized zymosan-stimulated monocytes (Fig. 5 *A* and *E*). These results suggest that ROCK2 is involved in p47phox phosphorylation in human monocytes.

ROCK2 Controls ROS Production in Human Monocytes and in THP1 Cell Line. To evaluate the role of ROCK2 in ROS production, isolated monocytes were treated as before with Y27632 or KD025, prior to stimulation with fMLF, PMA, or opsonized zymosan. The results showed that KD025 at 1 and 10 μM dramatically inhibited fMLF-, PMA- and opsonized zymosan-induced ROS production in monocytes (Fig. 6 *A* and *F*). Interestingly, ROCK2 inhibitors Y27632 or KD025, have no or a moderate effect on fMLF-, PMA- and opsonized zymosan-induced ROS production by human neutrophils (*SI Appendix*, Fig. S3). These results suggested that

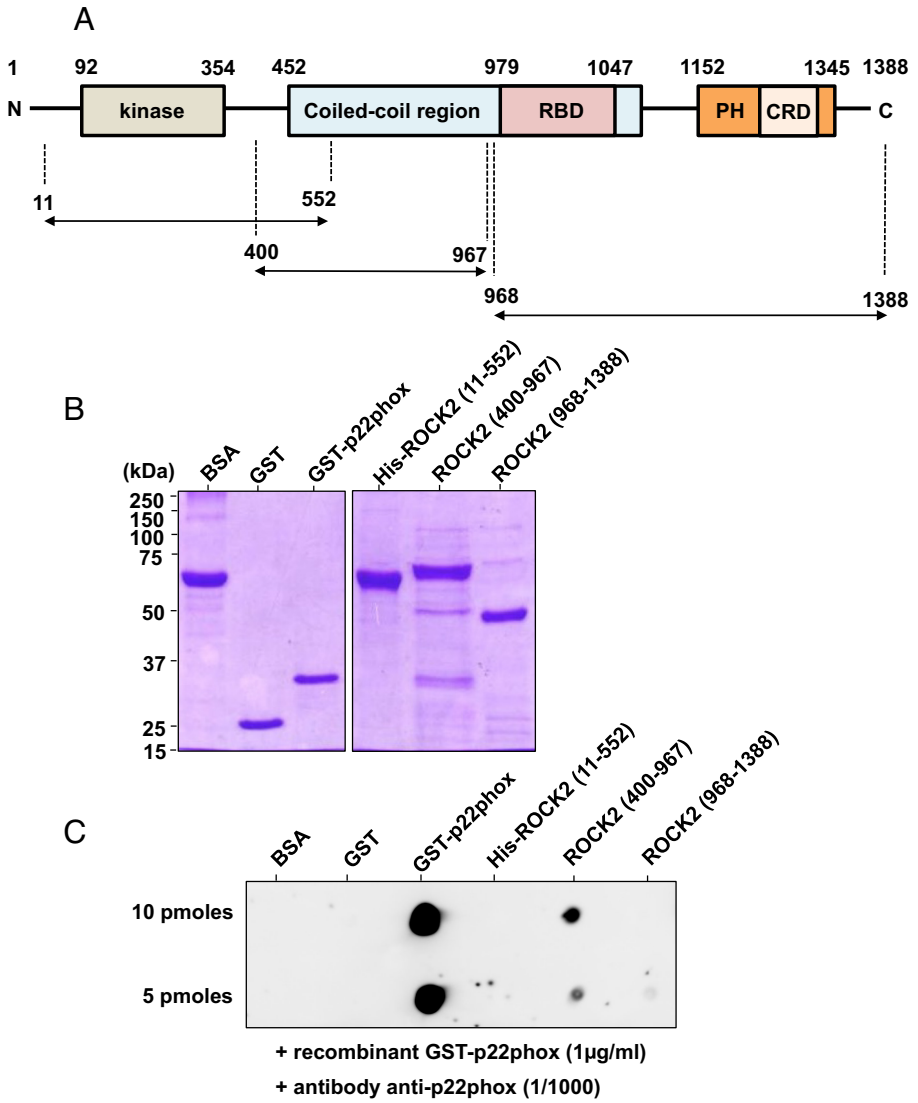

Fig. 2. ROCK2 interacts directly with p22phox through the coiled-coil region. (*A*) Schematic representation of ROCK2 and the different regions used for the interaction (amino acids 11 to 552), (amino acids 400 to 967), and (amino acids 968 to 1,388). RBD: Rho-binding domain; PH: pleckstrin homology domain; CRD: cysteine-rich C1 domain. (*B*) Coomassie blue staining of BSA, GST, recombinant GST-p22phox (132 to 195), His-ROCK2 (11 to 552), ROCK2 (400 to 967) and ROCK2 (968 to 1,388) expressed in *Escherichia coli* BL21. (*C*) Dot-blotting on nitrocellulose membranes of BSA, GST alone, recombinant GST-p22phox (132 to 195), His-ROCK2 (11 to 552), ROCK2 (400 to 967) or ROCK2 (968 to 1,388) probed with recombinant GST-p22phox (132 to 195). Interaction between the two partners was revealed with an anti-p22phox antibody and an HRP-conjugated secondary antibody. BSA and GST were used as negative controls. Dot-blot is a representative of three independent experiments.

ROCK2 is involved in NADPH oxidase activation in a cell-specific manner, including monocytes but not neutrophils.

To confirm the above results, we used a second approach to downregulate ROCK2 expression in THP1-monocytic cells. We first confirmed the expression of ROCK2 in THP1 cells, with the aid of specific monoclonal antibodies, obtaining similar to that found with human monocytes, lymphocytes, and neutrophils ; surprisingly, ROCK1 was less expressed in human monocytes, neutrophils and THP1 cells when compared with the expression in human lymphocytes (Fig. 7*A*). In addition, we showed that ROCK2 coimmunoprecipitated with p22phox in THP1 cells (Fig. 7*B*) and that ROCK2 inhibitors inhibited ROS production in THP1 cells (*SI Appendix*, Fig. S4). Furthermore, transfection of THP1 cells with a specific siRNA for ROCK2, not only decreased its protein level (Fig. 7 *C* and *D*) but also reduced ROS production induced by fMLF, PMA, and Op. Zymosan (Fig. 7*E*). The specificity for ROCK2 was further validated by the lack of inhibition of siRNA for ROCK1. These results strongly support the involvement of ROCK2 in NADPH oxidase activation and ROS generation in human monocytes.

Discussion

Monocytes play an important role in inflammation and in host defense against infection by activating the phagocytes NADPH oxidase and ROS production. Although the pathways involved in NADPH oxidase activation have been widely investigated in neutrophils, these pathways are less well known in other cells, such as monocytes and dendritic cells. In this study, we used coimmunoprecipitation and mass spectrometry techniques to identify p22phox-interacting proteins in human monocytes. We thus identified ROCK2 as a partner of p22phox in human monocytes. ROCK2 colocalized with p22phox in intact monocytes and phosphorylated the NADPH oxidase cytosolic component p47phox in vitro. ROCK2 inhibitors altered p47phox phosphorylation and NADPH oxidase activation in human monocytes. Furthermore,

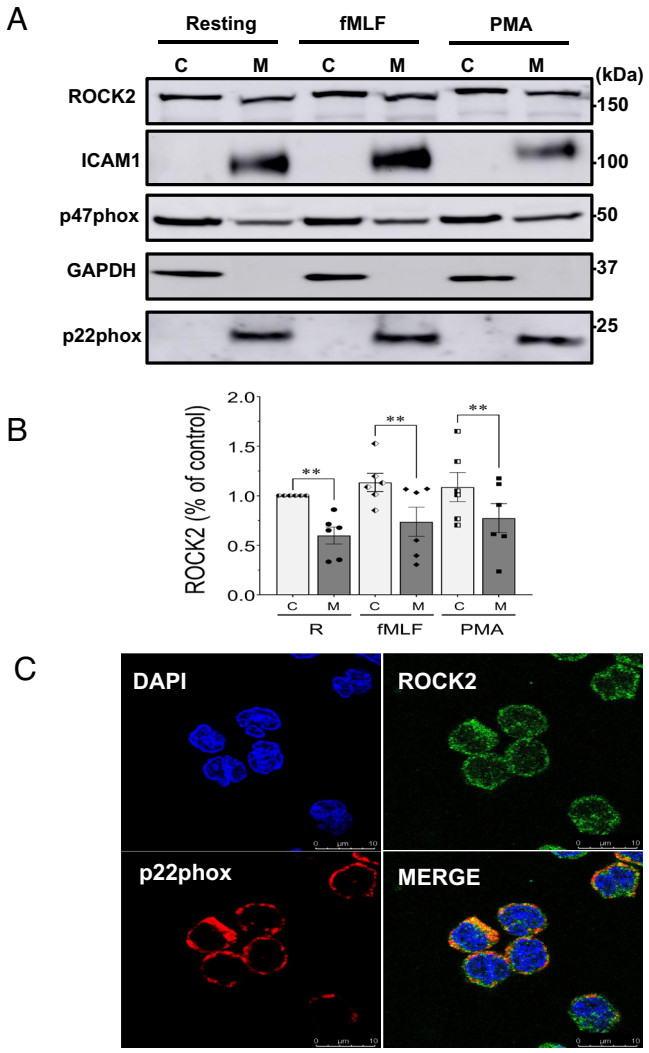

Fig. 3. ROCK2 localized in cytosol and membrane fractions and colocalized with p22phox in human monocytes. (*A*) Representative western blots of monocyte cytosol (C) and membrane (M) fractions isolated by differential centrifugation in resting cells or with stimulation by fMLF (10^{-6} M) for 10 s or PMA (100 ng/mL) for 10 min. After SDS-PAGE and western blots, proteins were detected using anti-ROCK2, anti-ICAM1, anti-p47phox, anti-GAPDH, and anti-p22phox antibodies. (*B*) ROCK2 protein bands of five experiments were quantified and membrane ROCK2 expressed as % of cytosolic ROCK2 in resting condition. Values are mean ± SEM of three independent experiments and were analyzed by one-way ANOVA with Tukey's multiple comparisons test. $^{**}P < 0.01$, compared ROCK2 in cytosol. (*C*) Confocal microcopy of resting monocyte cells labeled with DAPI (blue), anti-ROCK2 (green), and anti-p22phox (red). 63X objective, zoom 4X. Representative example of two independent experiments.

inhibition of ROCK2 expression using siRNA in THP1 monocytic cells inhibited ROS production.

The ROCK1/2 proteins are known to be expressed in human monocytes, dendritic cells, neutrophils, and monocytic cell lines such as THP1 and U937 (35–37). Here, we show that these myeloid cells express mainly the ROCK2 isoform, while ROCK1 is less expressed. ROCK1/2 are involved in several key monocyte functions, such as migration, adhesion, and differentiation into macrophages (25, 35, 36). However, the role of ROCK2 in NADPH oxidase activation and ROS production in monocytes is unknown. In the present study, we show that ROCK2 coimmunoprecipitated with p22phox in monocytes and directly interacted with the cytosolic tail of p22phox (amino acids 132 to 195) in vitro via its coiled-coil domain (amino acids 400 to 967), which is close to the RBD (amino acids 979 to 1,047). ROCK1 and ROCK2 overall identity is 64%, with 90% identity in the kinase domain, but only 55% identity in the coiled-coil region RBD domain and 65% identity in the PH domain (18, 21). Our data are strongly in favor for a role of ROCK2, rather than ROCK1 in monocyte ROS production. First, mass spectrometry demonstrated that 30 out of 34 peptides belong to ROCK2 sequence, with only four peptides being in common to ROCK2 and ROCK1, and none fully specific for ROCK1. Secondly, the Mascot score of ROCK2 was 363, in contrast the one of ROCK1, 18 was similar to the one found in the immunoprecipitates with control IgG. Finally, transfection of THP1-monocytic cells with a specific siRNA for ROCK2, decreased its protein level and reduced ROS production induced by fMLF, PMA, and Op. Zymosan, while no effects were observed with ROCK1 siRNA.

We found that ROCK2 and p22phox shared the same membrane compartment in monocytes, with ROCK2 being present also in the cytosol. ROCK2 localization in the cytosol and membrane fractions of resting monocytes did not change after stimulation of cells with fMLF or PMA. However, the molecular weight of ROCK2 was slightly lower in the membrane fraction, may be due to its cleavage, which induces constitutive activation of ROCK2, as described by Sebbagh et al. (38). Indeed, we found that ROCK2 was constitutively active in resting monocytes (*SI Appendix*, Fig. S2). Although, Sebbagh et al. (38) showed that granzyme B was responsible for ROCK2 cleavage, we were not able to detect granzyme B in resting monocytes, therefore we hypothesize that a different protease could cleave ROCK2.

Activated ROCK2 phosphorylates several target proteins, such as myosin light chain (MLC), MLC phosphatase1 (MYPT1), LIMKinase, adducing ezerin radixin moesin (ERM), vimentin, MARKS, calponin, PTEN, and many other proteins (18, 39, 40). Based on these studies and other ROCK2 substrates, the consensus amino acid sequence for ROCK2 was found to be "Arg/Lys-X-X-Ser/Thr" or "Arg/Lys-X-Ser/Thr" (18, 40). In this study, we show that ROCK2 also phosphorylates human p47phox on Ser304, Ser315, Ser320, and Ser328. Indeed, these phosphorylated serines are located in the known ROCK2 consensus amino acid sequence RRS(S304*)IRNAHSIHQR(S315*)RKRL(S320*)QDAYRRN(S328*)VRF. Interestingly, ROCK1/2 inhibitors, such as Y27632 and KD025, altered the phosphorylation of p47phox on serine 304, 315, 320, and 328 in intact monocytes stimulated with fMLF and opsonized zymosan, suggesting the involvement of ROCK2 in p47phox phosphorylation in monocytes. KD025 also inhibited superoxide production by monocytes and siRNA for ROCK2 confirmed this effect in THP1-monocytic cells, thus supporting the involvement of ROCK2 in NADPH oxidase activation in these cells.

It is noteworthy that despite the binding of ROCK2 to p22phox, ROCK2 did not phosphorylate p22phox or the other NADPH oxidase components (p40phox, p67phox, and gp91phox). However ROCK2 phosphorylates p47phox, suggesting that p22phox is a docking site for ROCK2 to bring it close to its substrate p47phox. In addition to ROCK2, several other protein kinases, such as PKC, PKA, AKT, and PAK, phosphorylate p47phox at the same sites (8). These protein kinases can be activated in different phagocytes depending on the agonist used and thus can phosphorylate p47phox to regulate NADPH oxidase activation and phagocyte ROS production. Indeed, it was suggested that ROCK1/2 can phosphorylate p47phox on Ser345 and can amplify superoxide production to maintain a positive feedback loop for ROS generation in A549 epithelial cells (41).

In summary, our results suggest a mechanism for p47phox phosphorylation and NADPH oxidase activation in human monocytes; in resting monocytes ROCK2 is constitutively active and binds to p22phox via its coiled-coil region and to membrane

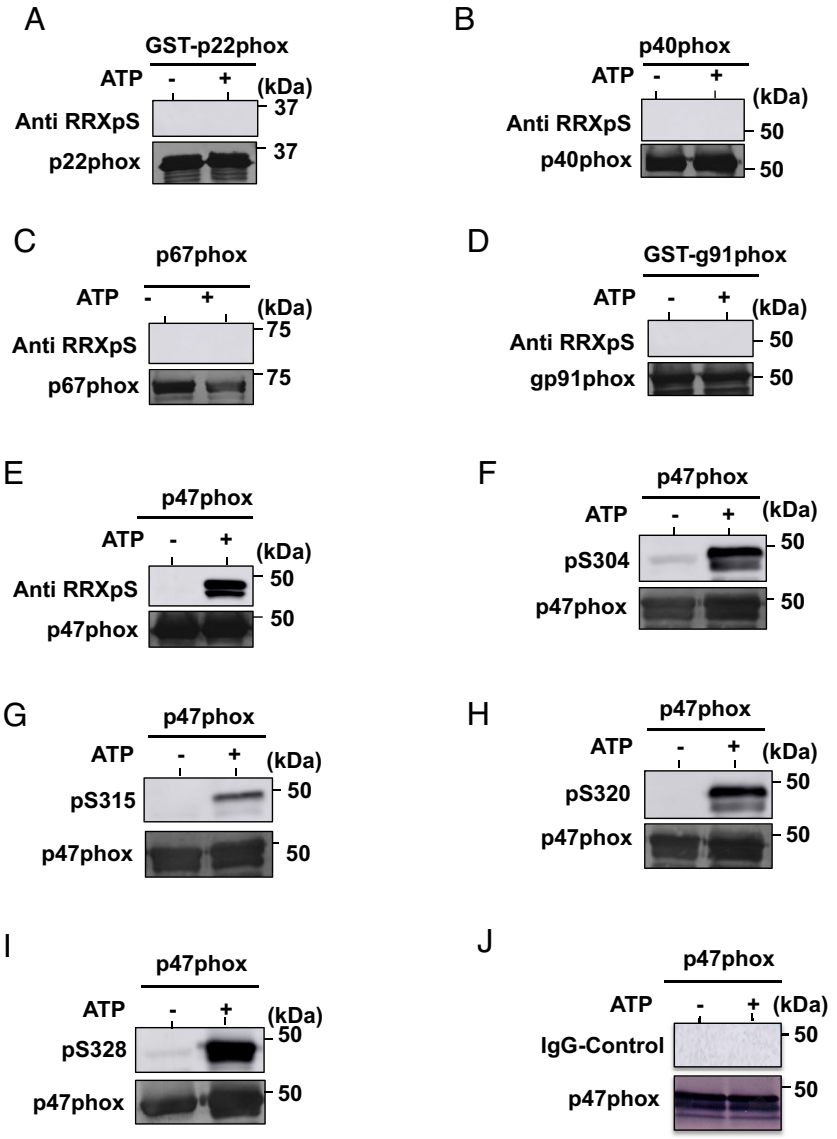

Fig. 4. ROCK2 phosphorylates p47phox but not p22phox, p40phox, p67phox, or gp91phox. Representative western blots of the recombinant proteins GST-p22phox (amino acids132-195) (*A*), p40phox (*B*), p67phox (*C*), GST-gp91phox (amino acids 291 to 570), (*D*) and p47phox (*E*) phosphorylated by constitutively active His-ROCK2 in the presence or absence of cold ATP. Blots were incubated with anti-phospho-(RRXS/Thr) substrate. Total p22phox (*A*), p40phox (*B*), p67phox (*C*), gp91phox (*D*), and p47phox (*E*) antibodies were used as controls for protein loading and transfer. Phosphorylation of p47phox was analyzed by western blot using phospho-p47phox S304 (*F*), S315 (*G*), S320 (*H*), S328 (*I*), and control IgG antibodies (*J*). Total p47phox antibody was used as a control for protein loading and transfer. Representative example of three independent experiments.

phospholipids via its PH domain, while p47phox is not phosphorylated in the cytosol of resting cells. Following monocyte activation, a first phosphorylation step of p47phox in the cytosol by a PKC isoform, induces its binding to p22phox via the p47phox-SH3 domain-p22phox-Pro rich region (PRR). This interaction will bring p47phox close to the active ROCK2, which phosphorylates translocated p47phox in the membrane.

In conclusion, the results presented here identified an interaction between p22phox and ROCK2 in monocytes and showed that ROCK2 is involved in p47phox phosphorylation and ROS production in human monocytes. ROCK2 could represent a therapeutic target in inflammatory diseases involving monocytes.

Materials and Methods

Reagents. Dextran T500 and Ficoll were purchased from GE Healthcare. Dulbecco's phosphate-buffered saline (PBS), bovine serum albumin (BSA), Hanks' balanced salt solution (HBSS), fMLF, PMA, ATP, luminol (5-amine-2,3-dihydro-1,4-phtalazinedione), Y27632, KD025, and all the other chemical products used were obtained from Sigma Aldrich. Human granulocyte/macrophage colony-stimulating factor (GM-CSF), and interleukin-4 (IL-4) were obtained from PeproTech France. Sodium dodecyl sulfate-polyacrylamide gel electrophoresis (SDS–PAGE) and western blot reagents were purchased from Bio–Rad (Marnes-la-Coquette, France). ROCK2 cDNA and active ROCK2 protein were purchased from the University of Dundee, School of Life Sciences Medical Sciences Institute, Scotland. Antibodies against phospho-(R-RXS/Thr)-PKA substrate (mab#9624) and ROCK2 (used for IP: D1B1#9029) were from Cell Signaling Technology. An anti-ROCK2 antibody (used for IP#20248-1-AP) was from Proteintech. Antibodies against ROCK2 (D11, sc-398519), ROCK1(G6, sc-17794), ICAM1 (G5, sc-8439), GADPH (6C5, sc-32233), p40phox (B-1, sc-48376), and gp91phox (54.1, sc-130543) and secondary antibodies were purchased from Santa Cruz Biotechnology. Rabbit polyclonal antibodies against p47phox, p22phox, and p67phox and phosphorylated p47phox-sites were generated by our lab as previously described (32, 33, 42).

Ethics Statement. Venous blood was obtained from healthy volunteers after written informed consent was obtained. The study was approved by the institutional review boards (IRBs) and ethics committee of Institut national de la santé

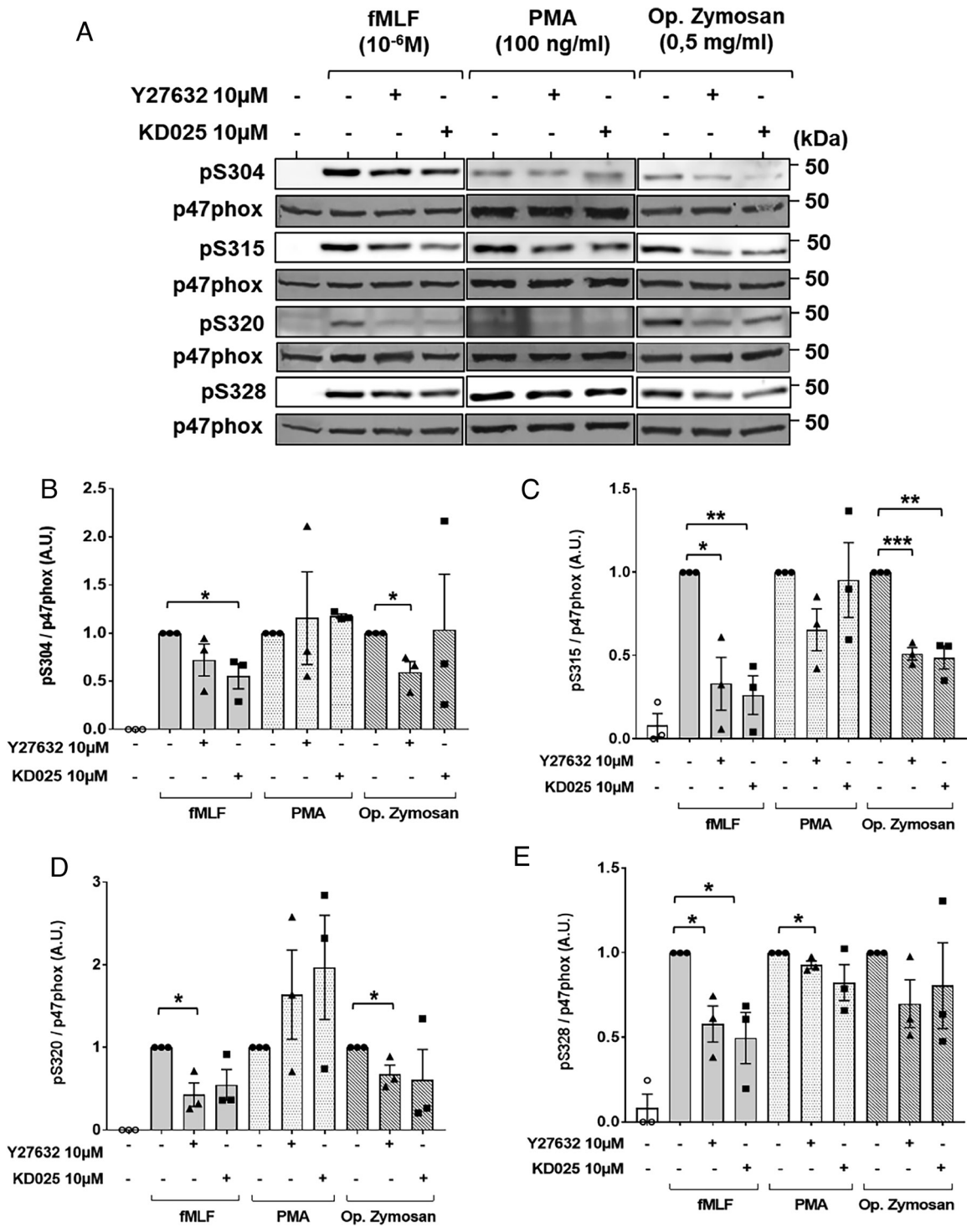

Fig. 5. Effect of Y27632 and KD025 on fMLF-, PMA- and opsonized zymosan-induced p47phox phosphorylation in human monocytes. (*A*) Monocytes (2×10^6) were not treated or (First line) or treated with fMLF (10^{-6} M) for 10 sec, PMA (100 ng/mL) for 10 min or opsonized zymosan (0.5 mg/mL) for 5 min at 37 °C in the absence or presence of Y27632 or KD025 at 10 μM and lysed with Laemmli sample buffer. Phosphorylation of p47phox was analyzed by western blot using phospho-p47phox- S304, -S315, -S320 and -S328 antibodies. Total p47phox antibody was used as a control for protein loading. Western blots are a representative example of three independent experiments. (*B*–*E*) Quantitative analysis of phospho-p47phox -S304 (*B*), -S315 (*C*), -S320 (*D*), and -S328 (*E*) normalized to p47phox expression. Values are mean ± SEM of three independent experiments and were analyzed by one-way ANOVA with Tukey's multiple comparisons test. $^{**}P < 0.01$, $^{***}P < 0.001$ compared with the control in fMLF, PMA, or opsonized zymosan stimulation (1 A.U.).

et de la recherche médicale (INSERM) (EFS convention number: 2018010827). All these procedures were conducted in accordance with the 1975 Declaration of Helsinki, as revised in 2013.

Human Monocyte, Lymphocytes, and Neutrophil Isolation. Cells were isolated by dextran sedimentation and Ficoll centrifugation. Peripheral blood mononuclear cells (PBMCs) were washed and resuspended in PBS with 0.5% bovine serum albumin (BSA) and 1 mM EDTA to a 5×10^7 cells/mL final concentration. To isolate monocytes and lymphocytes from PBMCs, the cells were subjected to magnetic negative isolation with EasySep™ Human Monocyte Isolation (Stemcell Technologies) following the manufacturer's instructions (43). After Ficoll centrifugation, the pellet was recovered and red blood cells were lysed, neutrophils in the pellet were washed, and resuspended in HBSS.

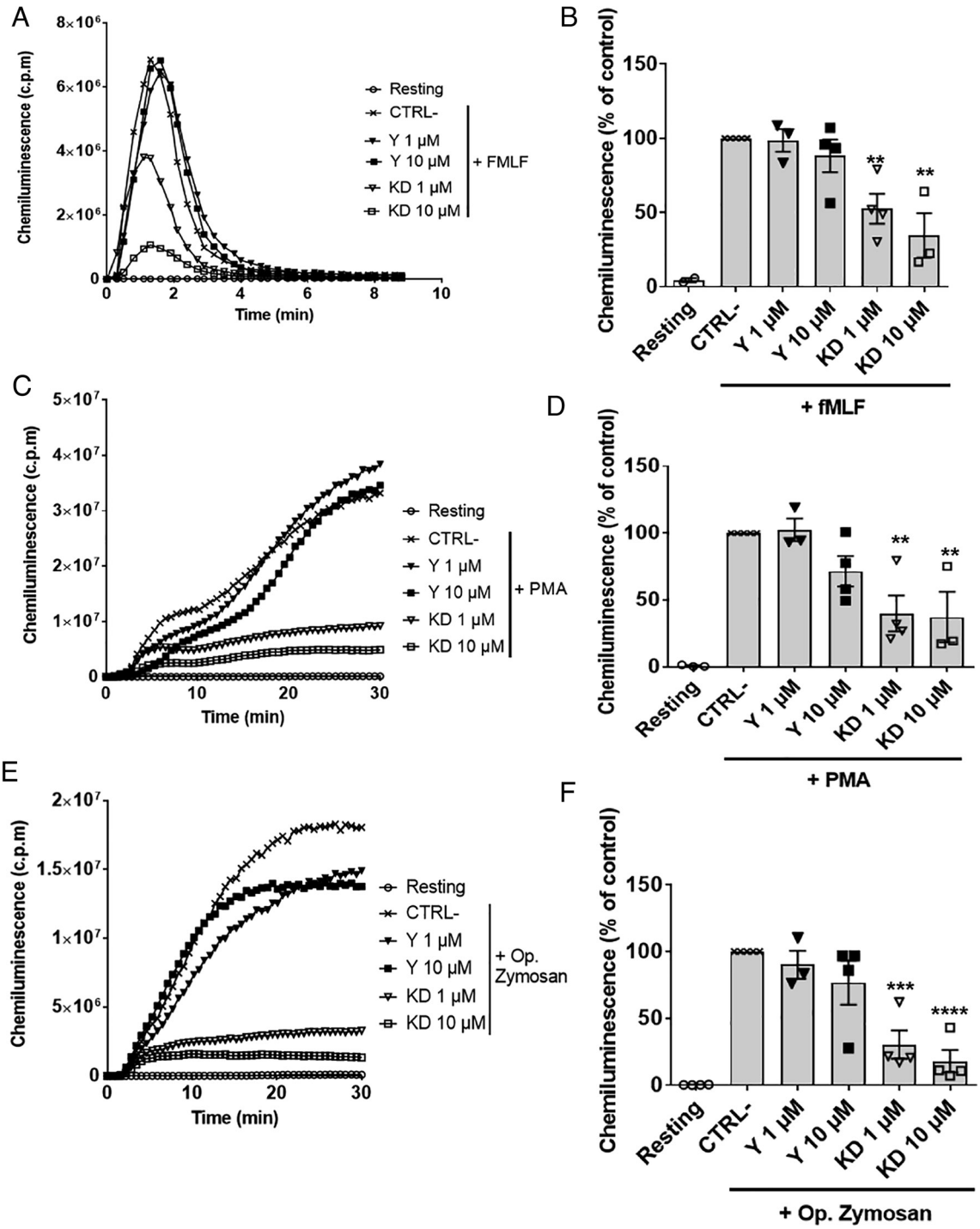

Fig. 6. Effect of Y27632 and KD025 on fMLF, PMA and opsonized zymosan-induced ROS production in human monocytes. Monocytes (5×10^5) were resuspended in HBSS (0.5 mL) and preincubated for 30 min at 37 °C in the presence of luminol (10 µM) with or without Y27632 (1 or 10 µM) or KD025 (1 or 10 µM), cells were then stimulated with fMLF (10^{-6} M) for 10 min (*A* and *B*), PMA (100 ng/mL) for 30 min (*C* and *D*) or opsonized zymosan (0.5 mg/mL) for 30 min (*E* and *F*). The light emission is expressed in c.p.m. (*A*, *C*, and *E*) show the results of one representative experiment. (*B*, *D*, and *F*) show a quantification analysis of three independent experiments. Values (mean ± SEM of three independent experiments) are expressed as the percentage of the negative control (monocytes stimulated without inhibitor) and were analyzed by one-way ANOVA with Tukey's multiple comparisons test. $^{**}P < 0.01$, $^{***}P < 0.001$, $^{****}P < 0.0001$ compared with the negative control (100%). CTL-: negative control; Y: Y27632; KD: KD025.

Purity and viability of cells were assessed as described in *SI Appendix*, *Materials and Methods*.

Monocyte Differentiation into Dendritic Cells. Monocyte-derived dendritic cell differentiation was obtained after 6 d culture of freshly isolated monocytes in complete RPMI 1640 medium (Thermo Fisher Scientific, Gibco™) supplemented with 10% heat inactivated fetal bovine serum and antibiotics (100 U/mL penicillin, 100 µg/mL streptomycin) in the presence of 50 ng/mL GM-CSF and 1,000 U/mL IL-4 in 6-well tissue culture plates to a final concentration of 1.25×10^6 cells/mL (43). Differentiation of monocytes into DC and viability were assessed using a flow cytometer as described above using the following antibodies: anti-CD14 FITC/CD86PE/ CD209 PerCP-Cy5.5.

Coimmunoprecipitation of Proteins, SDS–PAGE and Mass Spectrometry. Cells (5×10^6) were lysed in 200 µL lysis buffer (10 mM Hepes, pH7.5, 10 mM NaCl, 100 mM KCl, 20 mM NaF, 5 mM G-phosphate, 0.1 mM DTT, 1.66 mM

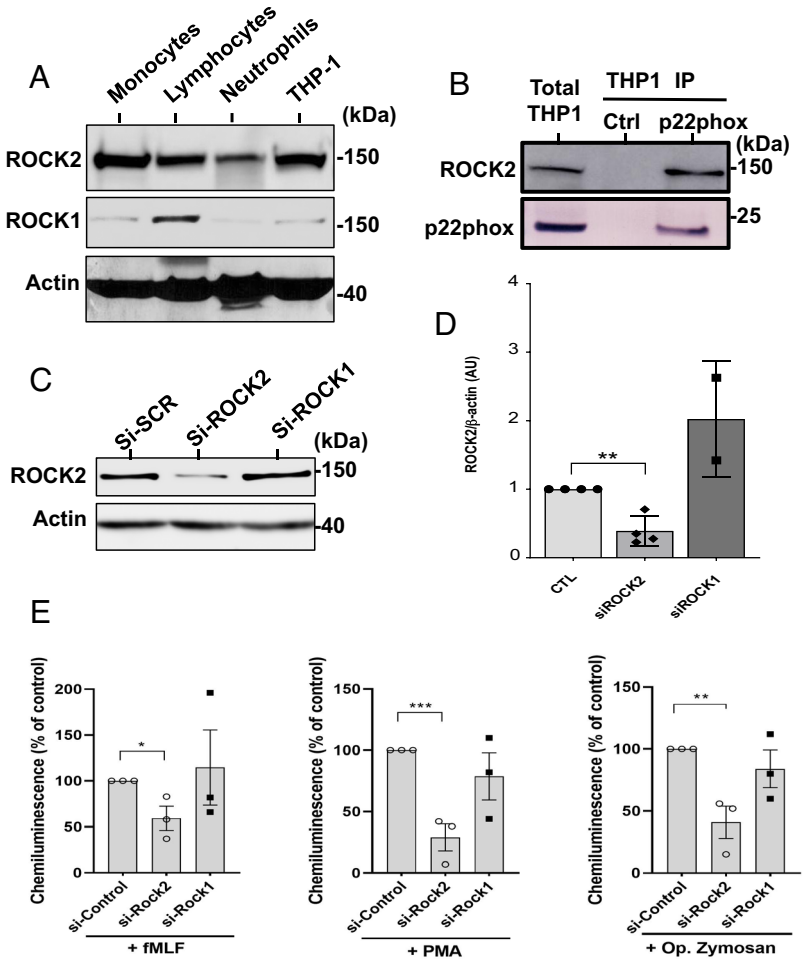

Fig. 7. Expression of ROCK2 and ROCK1 in THP1-monocytic cell line and the effect of siRNA. (*A*) Western blot of ROCK2, ROCK1 and β-actin in human monocytes, lymphocytes, neutrophils, and THP1. (*B*) Representative western blots of coimmunoprecipitation (co-IP) of ROCK2 with p22phox THP1. The p22phox-immunoprecipitated fraction (IP-p22phox) and IP-IgG-control-immunoprecipitated fractions (IP-IgG-Ctrl) were analyzed by SDS-PAGE and western blots and proteins detected with anti-ROCK2 and anti-p22phox antibodies. The total THP1 shows ROCK2 and p22phox protein levels. (*C*) THP1 cells were transfected with ROCK2- or ROCK1-siRNA, and ROCK2 and actin were detected by SDS-PAGE and western blots. (*D*) Quantification analysis of ROCK2 normalized to actin expression. (*E*) THP1 cells were transfected with ROCK2- or ROCK1-siRNA, and ROS production was measured using luminol-amplified chemiluminescence after stimulation with fMLF, PMA, and opsonized zymosan. Values are mean ± SEM of three independent experiments and were analyzed by one-way ANOVA with Tukey's multiple comparisons test. $^{**}P < 0.01$, $^{***}P < 0.001$ compared with si-control. Western blots are representative examples of three independent experiments.

levamisole, 1% Protease inhibitors coctail, 2% Triton X-100, 1 mM PMSF), sonicated on ice (3 × 5 s) and centrifuged at 100,000 g for 30 min at 4 °C (44, 45). The supernatants were diluted twice in lysis buffer without Triton, incubated with a rabbit anti-p22phox antibody or rabbit IgG control for 2 h at 4 °C, and then incubated with protein A/G agarose for an additional 2 h at 4 °C. After three washes by centrifugation, the beads were resuspended in 1× Laemmli sample buffer (10% glycerol, 2.5% sodium dodecyl sulfate (SDS), 5% beta-mercaptoethanol, 62.5 mM Tris-HCl pH 6.8, 2.5 mM EDTA, 2.5 mM EGTA, 0.15 mM bromophenol blue, protease and phosphatase inhibitors), and denatured for 3 min at 100 °C. Proteins were analyzed by SDS–PAGE, cleaved in the gel, and analyzed by mass spectrometry (*SI Appendix*, Materials and Methods).

Cloning, Expression, and Purification of Recombinant Proteins. These methods are described in detail in (*SI Appendix*, *Materials and Methods*).

Protein Interaction by Dot-Blot Analysis. Recombinant proteins GST-p22phox (132 to 195), His-ROCK2 (11 to 552), ROCK2 (400 to 967), and ROCK2 (968 to 1,388) were diluted in PBS at 5 pmol/5 μL and 10 pmol/5 μL and were blotted onto nitrocellulose membranes dropwise in a delimited area. For the negative control, BSA and GST were used at the same concentrations. The nitrocellulose membrane was dried for 30 min at room temperature and blocked for 1 h at room temperature in 5% nonfat dry milk diluted in TBS-Tween (20 mM Tris-HCl pH 7.6, 137 mM NaCl, 0.05% Tween 20). Then, the membrane was probed overnight at 4 °C with the recombinant protein GST-p22phox (1 μg/mL) diluted in TBS-Tween containing 1% nonfat dry milk. Three 5-min washes with TBS-Tween were performed, and the membrane was incubated with mouse anti-p22phox antibody (1:1,000) for 1 h at room temperature. After an additional three washes, the membrane was incubated with horseradish peroxidase-conjugated goat anti-mouse antibody (1:10,000) for 45 min at room temperature. After additional washes, the protein interaction spots were visualized using enhanced chemiluminescence western blotting reagents, and blots were visualized using a Amersham Imager 600 camera (GE Healthcare LifeSciences).

Preparation of Monocyte Cytosols and Membranes. Monocytes (10×10^6) resuspended in HBSS (500 μL) were stimulated at 37 °C with or without fMLF (10^{-6} M) for 10 s or PMA (100 ng/mL) for 10 min. The stimulation was stopped by adding ice-cold PBS, and cells were pelleted by centrifugation. The pellet was lysed by sonication on ice (3 × 10 s) in relaxation buffer containing 10 mM PIPES (pH 7.3), 100 mM KCl, 3 mM NaCl, 3.5 mM $MgCl_2$, 1 mM ATP, 1 mM EGTA, 1.5% protease inhibitor cocktail, 0.5 mM PMSF, and 0.1 mM DFP (46). To separate the cytosol and the membrane proteins, the lysates were centrifuged at 100,000 g for 1 h at 4 °C. The supernatants containing the cytosolic proteins were recovered, and the membrane pellets were washed in relaxation buffer. All fractions were denatured for 3 min at 100 °C in 5× concentrated Laemmli sample buffer. The samples were stored at −80 °C until use for western blotting.

Confocal Microscopy. Resting monocytes (1×10^6 cells/100 μL) were fixed in suspension with 4% paraformaldehyde for 10 min and permeabilized with 90% methanol for 30 min at 4 °C (43). After centrifugation, the cells were resuspended in PBS, spun on slides using a cytospin centrifuge and blocked overnight with 1% PBS/BSA at 4 °C in a humidity chamber. Cells were then incubated for 1 h at room temperature with a rabbit anti-ROCK2 antibody (1:250) and a mouse anti-p22phox antibody (1:250) diluted in 1% PBS/BSA. After washing with 1% PBS/BSA, the cells were incubated with an Alexa Fluor 488 goat anti-rabbit antibody (1:500) and Alexa Fluor 555 goat anti-mouse antibody (1:500) for 45 min at room temperature in the dark followed by nuclear staining with DAPI solution (Thermo Fisher Scientific) at 1:1,000 for 10 min. The slides were mounted with ProLong™ Gold Antifade Mountant (Thermo Fisher Scientific) and examined with a Leica SP8 confocal microscope.

In Vitro Phosphorylation Assay. Briefly, 30 μM recombinant proteins GST-p22phox (132 to 195), p40phox, p67phox, GST-gp91phox (291 to 570), and p47phox was incubated with 0.15 μM constitutively active catalytic domain of ROCK2 (11 to 552) in the absence or presence of ATP (100 μM). The reaction was performed at 30 °C for 15 min in 50 μL reaction buffer containing 50 mM Tris-HCl (pH 7.5), 10 mM DTT, 0.1 mM EGTA, and 10 mM $MgCl_2$. The reaction was stopped by adding 5× concentrated Laemmli sample buffer, and the samples were denatured for 3 min at 100 °C and stored at −80 °C until use for western blotting.

Monocyte Treatment for Western Blotting Analysis. Monocytes (2×10^6) resuspended in HBSS (100 μL) were treated with Y27632 or KD025 (10 μM) for 30 min at 37 °C with mild shaking. The stimulation was performed at 37 °C with fMLF (10^{-6} M) for 10 s, PMA (100 ng/mL) for 10 min or opsonized zymosan (0.5 mg/mL) for 5 min. The reaction was stopped by adding 5× concentrated Laemmli sample buffer, denatured for 3 min at 100 °C, sonicated, subjected to 10% SDS–PAGE (equivalent of 4.5×10^5 cells/well) and then analyzed by western blots using protein-specific antibodies.

Western Blot. After SDS–PAGE, the separated proteins were transferred to nitrocellulose, blocked for 1 h at room temperature in TBS-Tween containing 5% nonfat dry milk (42). Blots were incubated overnight at 4 °C with an anti-phospho-(RRXS/Thr) PKA substrate (1:1,000) or primary antibody: anti-ROCK2 (1:1,000), anti-β-actin (1:10,000), anti-p22phox (1:4,000), anti-p47phox (1:4,000), anti-p40phox (1:4,000), anti-p67phox (1:4,000), anti-gp91phox (1:4,000), anti-phospho-S304-p47phox (1:2,000), anti-phospho-S315-p47phox (1:2,000), anti-phospho-S320-p47phox (1:2,000), and anti-phospho-S328-p47phox (1:2,000). The membranes were washed with TBS-Tween and incubated with horseradish peroxidase-conjugated goat anti-rabbit or anti-mouse antibodies for 1 h at room temperature (1:10,000). After additional washes, the protein bands were revealed by a chemiluminescence method with ECL western blotting reagents and then visualized using a Amersham Imager 600 camera. Alternatively, the membranes were incubated with an alkaline phosphatase-conjugated goat anti-mouse or goat anti-rabbit antibody, and proteins were revealed with NBT/BCIP reagents (Sigma Aldrich) in carbonate buffer (100 mM $NaHCO_3$, 2 mM $MgCl_2$, pH 9.8). Antibodies against actin and total p22phox, p47phox, p40phox, p67phox, and gp91phox were used as controls for protein loading and transfer.

Measurement of ROS Production by Luminol-Amplified Chemiluminescence. Monocytes and THP1 cells (5×10^5) were suspended in 0.5 mL HBSS containing 10 μM luminol and preincubated for 30 min at 37 °C with or without Y27632 (1 or 10 μM) or KD025 (1 or 10 μM), two different ROCK2 inhibitors. ROS production was measured at 37 °C after the addition of fMLF (10^{-6} M) for 10 min, PMA (100 ng/mL) for 30 min, or opsonized zymosan (0.5 mg/mL) for 30 min (47). Luminol-amplified chemiluminescence was recorded with a luminometer (Berthold-Biolumat LB937). Light emission was expressed in counted photons per minute (c.p.m.).

THP1 Culture and Transfection. THP1 monocytic cell line was purchased from the American Tissue Culture Collection (ATCC). Cells were cultured in RPMI1640 medium supplemented with 10% fetal bovine serum and 1% penicillin/streptomycin. Cells were transfected with control (sc-37007) or ROCK2 siRNA (sc-29474) or ROCK1 (sc-29473) using reagents and protocol provided by Santa Cruz Biotechnology. After 48 h, the cells were washed and tested for ROS production and lysed in Laemmli sample buffer for SDS-PAGE and western blots.

Statistical Analysis. All results are expressed as mean ± SEM. Data were analyzed using GraphPad Prism 7 software (GraphPad Software). For two-group comparisons, unpaired *t* tests were used. One-way ANOVA with a Tukey's multiple comparison posttest was used for comparisons of more than three groups. $*P < 0.05$, $**P < 0.01$, $***P < 0.001$, $****P < 0.0001$ values were considered significant.

Data, Materials, and Software Availability. All study data are included in the article and/or *SI Appendix*.

ACKNOWLEDGMENTS. This study was supported by grants from Laboratoire d'Excellence Inflamex, Institut national de la santé et de la recherche médicale (INSERM), Centre national de la recherche scientifique (CNRS), University of Paris-Cité and Vaincre la mucoviscidose (VLM).

Author affiliations: [a]Institut national de la santé et de la recherche médicale (INSERM) U1149, Centre national de la recherche scientifique (CNRS) Equipe de recherche labellisée (ERL) 8252, Centre de Recherche sur l'Inflammation, Université de Paris-Cité, Laboratoire d'Excellence Inflamex, Faculté de Médecine Xavier Bichat, Paris F-75018, France; [b]Departement d'Immunologie et d'Hématologie, Unité Dysfonctionnements Immunitaires, Centre Hospitalo-Universitaire Xavier Bichat, Paris F-75018, France; [c]State key Laboratory of Cancer Biology, National Clinical Research Center for Digestive Diseases and Xijing Hospital of Digestive Diseases, Fourth Military Medical University, Xi'an 710032, China; and [d]Molecular Rheumatology, School of Medicine, Trinity Biomedical Sciences Institute, Trinity College Dublin, Dublin D02-R590, Ireland

1. C. Kantari, M. Pederzoli-Ribeil, V. Witko-Sarsat, The role of neutrophils and monocytes in innate immunity. *Contrib. Microbiol.* **15**, 118–146 (2008).
2. C. Shi, E. G. Pamer, Monocyte recruitment during infection and inflammation. *Nat. Rev. Immunol.* **11**, 762–774 (2011).
3. W. M. Nauseef, The phagocyte NOX2 NADPH oxidase in microbial killing and cell signaling. *Curr. Opin. Immunol.* **60**, 130–140 (2019).
4. C. C. Winterbourn, Reconciling the chemistry and biology of reactive oxygen species. *Nat. Chem. Biol.* **4**, 278–286 (2008).
5. A. Pizzolla *et al.*, Reactive oxygen species produced by the NADPH oxidase 2 complex in monocytes protect mice from bacterial infections. *J. Immunol.* **188**, 5003–5011 (2012).
6. P. V. Vignais, The superoxide-generating NADPH oxidase: Structural aspects and activation mechanism. *Cell. Mol. Life Sci.* **59**, 1428–1459 (2002).
7. J. El-Benna, P. M. Dang, M. A. Gougerot-Pocidalo, C. Elbim, Phagocyte NADPH oxidase: A multicomponent enzyme essential for host defenses. *Arch. Immunol. Ther. Exp. (Warsz.)* **53**, 199–206 (2005).
8. S. A. Belambri *et al.*, NADPH oxidase activation in neutrophils: Role of the phosphorylation of its subunits. *Eur. J. Clin. Invest.* **48**, e12951 (2018).
9. J. El-Benna, P. M. Dang, M. A. Gougerot-Pocidalo, J. C. Marie, F. Braut-Boucher, p47phox, the phagocyte NADPH oxidase/NOX2 organizer: Structure, phosphorylation and implication in diseases. *Exp. Mol. Med.* **41**, 217–225 (2009).
10. D. C. Thomas *et al.*, Eros is a novel transmembrane protein that controls the phagocyte respiratory burst and is essential for innate immunity. *J. Exp. Med.* **214**, 1111–1128 (2017).
11. G. A. Arnadottir *et al.*, A homozygous loss-of-function mutation leading to CYBC1 deficiency causes chronic granulomatous disease. *Nat. Commun.* **9**, 4447 (2018).
12. M. J. Stasia, CYBA encoding p22(phox), the cytochrome b558 alpha polypeptide: Gene structure, expression, role and physiopathology. *Gene.* **586**, 27–35 (2016).
13. S. Noreng *et al.*, Structure of the core human NADPH oxidase NOX2. *Nat Commun.* **13**, 6079 (2022).
14. F. R. DeLeo *et al.*, Processing and maturation of flavocytochrome b558 include incorporation of heme as a prerequisite for heterodimer assembly. *J. Biol. Chem.* **275**, 13986–13993 (2000).
15. T. L. Leto, A. G. Adams, I. de Mendez, Assembly of the phagocyte NADPH oxidase: Binding of Src homology 3 domains to proline-rich targets. *Proc. Natl. Acad. Sci. U.S.A.* **91**, 10650–10654 (1994).
16. H. Sumimoto *et al.*, Role of Src homology 3 domains in assembly and activation of the phagocyte NADPH oxidase. *Proc. Natl. Acad. Sci. U.S.A.* **91**, 5345–5349 (1994).
17. H. Sumimoto *et al.*, Structure, regulation and evolution of Nox-family NADPH oxidases that produce reactive oxygen species. *FEBS J.* **275**, 3249–3277 (2008).
18. L. Julian, M. F. Olson, Rho-associated coiled-coil containing kinases (ROCK): Structure, regulation, and functions. *Small GTPases.* **5**, e29846 (2014).
19. T. Shimizu *et al.*, Parallel coiled-coil association of the RhoA-binding domain in Rho-kinase. *J. Biol. Chem.* **278**, 46046–46051 (2003).
20. W. Wen, W. Liu, J. Yan, M. Zhang, Structure basis and unconventional lipid membrane binding properties of the PH-C1 tandem of rho kinases. *J. Biol. Chem.* **283**, 26263–26273 (2008).
21. O. Nakagawa *et al.*, ROCK-I and ROCK-II, two isoforms of Rho-associated coiled-coil forming protein serine/threonine kinase in mice. *FEBS Lett.* **392**, 189–193 (1996).
22. A. J. Ridley, Rho proteins, PI 3-kinases, and monocyte/macrophage motility. *FEBS Lett.* **498**, 168–171 (2001).
23. H. Honing *et al.*, RhoA activation promotes transendothelial migration of monocytes via ROCK. *J. Leukoc. Biol.* **75**, 523–528 (2004).
24. S. Vemula, J. Shi, P. Hanneman, L. Wei, R. Kapur, ROCK1 functions as a suppressor of inflammatory cell migration by regulating PTEN phosphorylation and stability. *Blood* **115**, 1785–1796 (2010).
25. Y. Takeda *et al.*, ROCK2 Regulates Monocyte Migration and Cell to Cell Adhesion in Vascular Endothelial Cells. *Int. J. Mol. Sci.* **20**, 1331 (2019).

26. O. Grisk, Potential benefits of rho-kinase inhibition in arterial hypertension. *Curr. Hypertens. Rep.* **15**, 506–513 (2013).
27. K. Satoh, Y. Fukumoto, H. Shimokawa, Rho-kinase: Important new therapeutic target in cardiovascular diseases. *Am. J. Physiol. Heart. Circ. Physiol.* **301**, H287–H296 (2011).
28. T. M. Seccia, M. Rigato, V. Ravarotto, L. A. Calò, ROCK (RhoA/Rho Kinase) in Cardiovascular-Renal Pathophysiology: A Review of New Advancements. *J. Clin. Med.* **9**, 1328 (2020).
29. J. K. Liao, M. Seto, K. Noma, Rho kinase (ROCK) inhibitors. *J. Cardiovasc. Pharmacol.* **50**, 17–24 (2007).
30. J. H. Kang *et al.*, Peptide substrates for Rho-associated kinase 2 (Rho-kinase 2/ROCK2). *PLoS One.* **6**, e22699 (2011).
31. M. Amano *et al.*, Kinase-interacting substrate screening is a novel method to identify kinase substrates. *J. Cell Biol.* **209**, 895–912 (2015).
32. T. Boussetta *et al.*, The prolyl isomerase Pin1 acts as a novel molecular switch for TNF-alpha-induced priming of the NADPH oxidase in human neutrophils. *Blood* **116**, 5795–5802 (2010).
33. S. A. Belambri *et al.*, Impaired p47phox phosphorylation in neutrophils from patients with p67phox-deficient chronic granulomatous disease. *Blood* **139**, 2512–2522 (2022).
34. A. A. Birukova *et al.*, Role of Rho GTPases in thrombin-induced lung vascular endothelial cells barrier dysfunction. *Microvasc. Res.* **67**, 64–77 (2004).
35. L. Yang, F. Dai, L. Tang, Y. Le, W. Yao, Macrophage differentiation induced by PMA is mediated by activation of RhoA/ROCK signaling. *J. Toxicol. Sci.* **42**, 763–771 (2017).
36. A. Zanin-Zhorov, R. Flynn, S. D. Waksal, B. R. Blazar, Isoform-specific targeting of ROCK proteins in immune cells. *Small GTPases.* **7**, 173–177 (2016).
37. V. Niggli, Rho-kinase in human neutrophils: A role in signalling for myosin light chain phosphorylation and cell migration. *FEBS Lett.* **445**, 69–72 (1999).
38. M. Sebbagh, J. Hamelin, J. Bertoglio, E. Solary, J. Bréard, Direct cleavage of ROCK II by granzyme B induces target cell membrane blebbing in a caspase-independent manner. *J. Exp. Med.* **201**, 465–471 (2005).
39. K. Riento, A. J. Ridley, Rocks: Multifunctional kinases in cell behaviour. *Nat. Rev. Mol. Cell Biol.* **4**, 446–456 (2003).
40. S. Hartmann, A. J. Ridley, S. Lutz, The function of Rho-associated kinases ROCK1 and ROCK2 in the pathogenesis of cardiovascular disease. *Front. Pharmacol.* **6**, 276 (2015).
41. K. C. Cap, J. G. Kim, A. Hamza, J. B. Park, P-Tyr42 RhoA GTPase amplifies superoxide formation through p47phox, phosphorylated by ROCK. *Biochem. Biophys. Res. Commun.* **523**, 972–978 (2020).
42. S. A. Belambri, P. M. Dang, J. El-Benna, Evaluation of p47phox phosphorylation in human neutrophils using phospho-specific antibodies. *Methods Mol. Biol.* **1124**, 427–433 (2014).
43. V. Marzaioli *et al.*, NOX5 and p22phox are 2 novel regulators of human monocytic differentiation into dendritic cells. *Blood* **130**, 1734–1745 (2017).
44. H. Raad *et al.*, Regulation of the phagocyte NADPH oxidase activity: Phosphorylation of gp91phox/NOX2 by protein kinase C enhances its diaphorase activity and binding to Rac2, p67phox, and p47phox. *FASEB J.* **23**, 1011–1022 (2009).
45. H. Raad *et al.*, Phosphorylation of gp91phox/NOX2 in human neutrophils. *Methods Mol. Biol.* **1982**, 341–352 (2019).
46. S. N. Clemmensen, L. Udby, N. Borregaard, Subcellular fractionation of human neutrophils and analysis of subcellular markers. *Methods Mol. Biol.* **1124**, 53–76 (2014).
47. S. Bedouhène, F. Moulti-Mati, M. Hurtado-Nedelec, P.M. Dang, J. El-Benna, Luminol-amplified chemiluminescence detects mainly superoxide anion produced by human neutrophils. *Am. J. Blood Res.* **7**, 41–48 (2017).